

10. CALIBRATION

10.1 OVERVIEW

The calorimeter calibration and monitoring is designed to determine the absolute energy scale and monitor the calorimeter system for changes during the lifetime of the detector for offline corrections. Parts of this system will also be used for the relative timing of each calorimeter tower and to measure the linearity of each tower readout. Other parts of this system will be used during construction and assembly for quality control.

The HCAL has five distinct complementary systems for the calibration and monitoring. These are:

- a) Megatile scanner: focused gamma source to measure light yield of each tile of every megatile.
- b) Moving radioactive wire source: source tube(s) installed in every megatile that crosses every tile.
- c) Light injection (UV laser and blue LED): UV laser light injection into two layers of each wedge. UV laser and blue LED light injection into the decoder box which has the photodetectors.
- d) Test beam calibration: several individual wedges with muons and hadrons versus moving radioactive wire source for absolute energy calibration scale.
- e) Physics events in the completed detector including jets and muons.

The megatile scanner will measure the relative light yield of each tile to better than 1%. The moving wire source will track changes of each tile to better than 0.7%. The laser light injection into the tiles is complementary to the moving wire source. In the decoder box, it will also be used for the timing of the individual calorimeter towers and for linearity measurement. Both the moving wire source and laser light injection will track changes in signal strength. The radioactive source will transfer absolute single-hadron test beam calibrations to the calorimeter. The test beam and physics events will provide the ultimate jet energy calibration.

Magnetic field brightening of scintillator light is well determined for the HE modules where the only effect is due to the increase in the signal due to the increase of light yield of the scintillator. For the HB, the effect is more complex and will be computed by using both the test beam results (initial) and physics jet events (final).

Light yield changes are expected due to ageing of the scintillators, radiation damage and changes in the photodetector response. Due to lack of space the moving wire source will be permanently attached to only two layers of each wedge where measurements can be performed during off beam times. These two layers are the first one after the electromagnetic calorimeter and one in the middle of the wedge, layer 10 for HE and layer 9 (or the last layer of tower 17, in eta) for HB. No permanent wire source will be needed for HO. In addition, during periods when the CMS detector is open, each megatile (including HO) will be scanned by the moving wire source. Radiation damage of scintillators in HB and HO are minimal, but for $2 < |\eta| < 3$ in HE, the light yield will degrade by as much as 50% during the lifetime of the detector. To monitor and apply corrections to this eta region, each tower has four longitudinal segments and each segment has laser light injection to follow degradation. In addition one 20° wedge will have permanent wire source access to all four longitudinal segments for absolute measurement.

The calibration and the monitoring of the calorimeter wedges is a multi-step process as

10. CALIBRATION

follows:

- a) The measurement of light yield of each tile of every megatile before insertion into the calorimeter wedges. This step will use the megatile scanner that will measure each tile by a collimated narrow spread gamma source driven by a computer controlled X, Y motion. In addition each megatile will also be measured by the moving gamma wire source in a steel tube inside the megatile assembly.
- b) After insertion inside the calorimeter wedge, each megatile will again be scanned with the moving wire source. The two layers that have the UV laser connection will also be excited by the laser.
- c) A small fraction of the calorimeter wedges will be placed in the test beam for the absolute calibration.
- d) After assembling the calorimeter segments, but before closing the CMS, each megatile will again be scanned by the moving wire source. The two layers per wedge will also be checked with the UV laser. During this period each decoder box will be excited by both the UV laser and blue LED for timing as well as monitoring. The procedure with the moving wire source will be repeated (about once a year) during the periods when the detector is opened.
- e) After the start of taking data, but during the off beam times, the layers that have light injection and the source tubes permanently connected, will be scanned by the UV laser and, occasionally, by the moving wire source. These will track the radiation damage, as well as other damages. Also, the decoder box will be flashed with UV laser and LED for monitoring purposes.

Calibration of HO-B and HO-E is via the continuous flow of energy across boundaries, and by muons, as well as by occasional-access wire gamma source, LED light injection to the prototubes, and we are considering laser light injection to the tiles for timing calibration.

10.1.1 Calibration and monitoring systems

Below is a brief description of each calibration and monitoring system.

THE MEGATILE SCANNER: This system is described in chapter 6 where a pure Caesium-137 gamma source moves under computer control a few millimetres above the megatile assembly. Phototubes connected to various tiles via optical fibres will read and store the signal strength of each tile.

THE MOVING WIRE SOURCE SYSTEM: As described in chapter 6, each megatile has four built-in source tubes where a Caesium 137 radioactive source at the end of a "wire" can be remotely inserted all the way across every row of tiles. Since each tile is in a different tower, each tile can be read independently. Inside the detector, only the first and middle layer of each HB and HE wedge will connect permanently to the moving source driver. The rest of the layers (including HO) can only be scanned when CMS is opened up. In HE one wedge will have permanent source tube connection to all four longitudinal segments to monitor the radiation damage at high eta and to cross check the light injection into tiles.

UV LASER and LED INJECTION: On the megatile layers with laser option, one quartz fibre per ϕ segment will bring in the UV pulse. It will then be fanned out to every tile by 200 micron quartz fibres. In the decoder box, both the laser and the LED will be used to excite a Y11 wave shifter. From this wave shifter, 200 micron quartz fibres will be fed to each pixel of every photodetector. This allows monitoring of the gain of every pixel as well as timing of the towers.

TEST BEAM CALIBRATION: A small number of wedges will be placed in a test beam at CERN where hadron and muons of various energies will be used to determine absolute calibration between beam energy and light yield response to the moving wire source.

PHYSICS CALIBRATION: In the CMS detector, single tracked hadrons from taus, jet balancing and dijet resonances will be used for in situ calibrations, as discussed in chapter 10.7. Muons will be used to determine the response to minimum ionising particles, and to link the HO to the rest of the calorimeter.

The HF calorimeters made of quartz fibres and read by photomultiplier tubes are in a much harsher radiation environment and require continuous monitoring of the radiation damage. As described in chapter 10.4.7, the calibration and monitoring system for HF uses the UV laser, test beam and physics events. The laser pulse is wavelength shifted and fed into each PMT to monitor the gain. In addition, the wavelength shifted laser pulse is also fed into the back end of a test fibre near maximum irradiation dose area. The front end of the fibre is then curved back into another nearby slot and read at the back end by a PMT. This system will follow the radiation damage accurately. The absolute calibration is by means of test beam data of several modules. During data taking, jets produced in conjunction with known particles (e.g. Z's) will also be used to further improve the calibration. We are investigating the option of moving Co-60 gamma sources at the front face of the HF calorimeter and in longitudinal source tubes (parallel to the quartz fibres) to provide tower-to-tower relative normalisation, transfer testbeam calibrations, and provide direct scans of the fibre radiation damage profiles.

10.1.2 Discussion of choice of calibration techniques

The energy resolution of the CMS Hadron calorimeters is expected to have a constant term of ~5%. In order not to degrade this significantly, it is important that the tower-to-tower energy scales be known to better than 3%, and that any changes in calibration with time can be monitored quickly and frequently, with an accuracy of 1% or better. The absolute initial calibration will be accomplished using moving radioactive sources to transfer testbeam calibrations of a few wedges to the rest of the calorimeter. Eventually, absolute calibrations will be refined, and the jet energy scale more precisely established, by use of various in situ physics signals. Frequent gain monitoring will be accomplished by systems for injecting light to the phototransducers and to a few selected layers of scintillating tiles, and verified occasionally by use of the moving radioactive source system.

Additional functions of the light injection system include: to provide timing calibration signals for all towers, and to provide a series of light intensities to check or calibrate the linearity of each calorimeter channel. The proposed light injection system is uniquely suited to perform these two functions.

The use of the moving source system for Quality Control/Quality Assurance of the optical systems at construction and assembly time is discussed fully in chapter six. The technique of visiting every tile with a moving source is essential to QC/QA of the optical systems at all stages, from megatile construction to the initial assembled calorimeter. Later, the moving source can check in detail whether the response profile of a tower has changed, permitting an accurate recalibration.

Moving source capability to transfer absolute testbeam calibrations

It is important to have an initial absolute calibration which is independent of collisions, in order to set uniform trigger thresholds and collect collision data optimally. The moving

radioactive source is uniquely suited to do this. The initial absolute calibration is also important because in situ physics HCAL calibration using collider data will take time to collect, analyse, and understand. Initially equalising all towers in the HCAL to an accuracy of 2% for single particles also dramatically simplifies and speeds up the in-situ calibrations, since there are 144 towers at each location in η . Since collision-related data are expected to be azimuthally symmetric, only 17 different η values need to be studied in HB, for example, and data from all 144 towers at a given η can be lumped together.

The moving source strategy allows us to put only several wedges into the testbeam. The method requires measuring the source response of every tile in the calorimeter ("fingerprinting" each tower) and making a suitably shower-weighted sum over the tile source responses of each tower. The method has demonstrated a systematic accuracy of $\sim 2\%$ in source-beam comparisons, and permits not only the relative normalisation of all towers in the calorimeter, but also the absolute normalisation of the calorimeter relative to a few towers which have been calibrated in testbeams. Recent preliminary analysis of the CDF endplug EM calorimeter testbeam module, from which beam calibrations will be transferred to the rest of the calorimeter, shows rms agreement of $\sim 1.8\%$ between the electron beam response and the EM-shower-weighted sums of the source responses of tiles within towers.

The first link in this calibration chain is discussed in chapter six. At the QC/QA stage of megatile construction, we measure the response of every tile to a collimated Cs-137 gamma source and also to the uncollimated wire gamma source. The ratio is preserved in a calibration data base, and is used whenever a wire-source fingerprint is taken.

The wire source response depends on the lateral size of the tile, the location of the source tube, and in a nonlinear way on the thickness of the scintillator, whereas the collimated source excites all tiles in an essentially absolute way. The collimated gamma source excites all tiles in an equal amount, independent of position and lateral tile size. With the collimated source, tiles are excited in direct proportion to their thickness. This tracks the excitation of the tiles by shower particles.

Care has been taken in the design to ensure that the source tubes do not move relative to the scintillator when the megatiles are installed in the calorimeter. Thus the collimated/wire ratio will still be valid. We use the collimated/wire ratios to calculate an effective "collimated source fingerprint", which is then convolved with the average depth profile of hadronic showers to predict the relative response of every tower, and to relate the testbeam wedges to the rest of the calorimeter.

Variations in absorber thickness could, in principle, lead to shower response variations. The moving source technique does not address this source of variation, which could contribute to the rms seen in source/beam ratios for a set of towers, for example the above mentioned 1.8% rms seen at the CDF testbeam. For CMS HB and HE such absorber variations are not expected to cause significant degradation of the testbeam/source calibrations.

Magnetic brightening of scintillator in magnetic field

One essential link to complete the testbeam/source calibrations is to understand, and where possible measure in situ, the magnetic brightening effects at 4 Tesla[1]. The radioactive source has been shown to follow accurately the magnetic brightening of scintillator. Light injection cannot measure this brightening. The brightening curve for a particular type of scintillator is measured in advance, and can in principle be applied to zero-field calibrations if it

proves too difficult to run moving sources with the field on. The magnetic field is expected to be very uniform over all parts of HB and HE. In HO the field is less than 4 Tesla, but known, and corrections will be applied. We are pursuing the engineering development of a source driver using non-magnetic motors to permit direct field-on source measurements of one tile in every tower.

Magnetic shower energy steering in HB

The last link in the absolute calibration chain, relevant only for the HB configuration where the magnetic field is parallel to the HCAL plates, is the magnetic steering of extra shower energy into the scintillator. As discussed in chapter one, this effect has been predicted by GEANT and confirmed in the 1996 H2 testbeam measurements at CERN. The effect is predicted to be, and measured to be, absent in the HE configuration where the plates are perpendicular to the magnetic field. The radioactive gamma source is, of course, unable to measure this effect which involves the steering of charged particles. The effect depends on the placement of the scintillator package in the gap, and is minimised by placing the scintillator in the (radially) outer location in the gap. As discussed in chapter 1, there is a relatively large variation if the front and rear air gaps both change due to motion of the scintillator package in the slot. The present HB design uses venetian-blind springs to support the scintillator packages firmly to the outside of the 9 mm gap in the brass. For a 7 mm thick scintillator package in this location, GEANT calculations for 50 GeV pions show less than 2% increase in response at 4 Tesla — the HB baseline geometry happens to be rather close to optimal.

Tolerances in machining and in scintillator thickness are estimated to give an air gap of approximately 1.5 to 2 mm in front of the megatile package. GEANT calculations indicate 4%/mm change in response as a function of front air gap, for pions at 4 Tesla. Thus we expect an rms scatter of $(4\%/mm)(0.5mm)/\sqrt{12}$ or less than 1% in the pion shower steering factor at 4 Tesla, globally for all tiles in the HB. Therefore, we believe that the magnetic steering factor can be applied globally to the radioactive source calibration of HE, and that the resulting absolute single-hadron calibration will be accurate within the desired 3% systematic accuracy.

A further possible redundant cross-check of magnetic field effects can be done by collecting various classes of collider HCAL signals with the magnetic field on and off. Magnetic steering of the copious lower- momentum charged particles in jets (curl-up of tracks with $p_T < 800$ MeV/c in the tracking volume, oblique incidence of other charged particles onto the ECAL, and magnetic steering of showers between ECAL and HB) would need to be understood in order to use this technique. These issues relate to the field-on jet energy scale and will therefore need to be studied and understood in any case.

Source monitoring

The moving source system has a repeatability (as distinguished from systematic accuracy) of approximately 0.5%, and can be used, at relatively infrequent intervals, in the permanently accessible layers to monitor changes in the response of each tower. This will also serve to monitor and calibrate the more frequently used light injection to the phototubes and to the special megatiles.

10.2 SPECIFICATIONS AND REQUIREMENTS (HB/HE/HO/HF)

The calibration and monitoring system should be capable of establishing the initial calibration of every tower to an accuracy of 3%, and of maintaining calibrations to 1%

10. CALIBRATION

accuracy. The initial calibrations are necessary, among other reasons, to permit clean trigger thresholds at the start of collisions, to permit immediate use of the calorimeters for physics analysis, and as a cross check of possible in-situ calibrations done using physics signals from the collisions.

The light injection system should be capable of determining the relative timing of towers to a few ns. This system will also use a series of selectable neutral density filters, with a dynamic range of four orders of magnitude covering the dynamic range of the photodetectors and DAQ, to measure the linearity of each tower.

10.3 SOURCE CALIBRATIONS

Source calibrations involve, first, the use of movable collimated radioactive gamma sources in three megatitle scanner boxes, in conjunction with the use of three CDF-style wire source drivers. Then, at the testbeam, one or more further wire source drivers will take data for the transfer of testbeam calibrations to the HB, HE and HO (and possibly HF). Further wire source drivers will be used at the wedge assembly area and in the detector hall for late-stage QC/QA and then for "occasional access" sourcing of every tile.

Finally, three dedicated slimline wire source drivers will be installed on each half-barrel and each endcap, and coupled permanently to one scintillator layer in every tower of each HCAL depth compartment, thus permitting calibration monitoring by the sources when the detector is closed. This is a total of 12 permanently installed non-magnetic slimline source drivers for HB and HE. Prototype slimline source drivers are being developed in 1997, capable of fitting in the space between the back of a barrel wedge and the magnet cryostat. Development is also underway of piezoelectrically switched air motors capable of operating in a 4 T magnetic field, to permit field-on source calibrations of at least one tile in every tower, and thus measure directly the magnetic brightening of tiles in a variety of locations.

10.3.1 Design specifications

The design and use of wire source drivers and the associated systems are described[2,3,4,5,6,7,8]. The radioactive source is mounted inside the tip of a long flexible stainless steel "wire": a point-like Cs-137 gamma source, with active length typically 5 mm and activity in the range 0.5 to 5 mCi, is contained at one end of a sealed 22 gauge stainless steel needle-grade fully-hardened hypodermic tube, of 0.71 mm OD and with a length of up to about 11 m. The active element in future sources, manufactured by the Isotope Products Laboratory of Burbank, California, will be a set of ion exchange beads which have been sealed and hardened by heating in a Hydrogen atmosphere. An internal keeper wire holds the active element at one end of the sealed tube, which is a second level of source encapsulation. Further details are given in Chapter 6. The source is garaged in a cylindrical lead pig when not in use. The wire is coiled in a storage reel of radius 12.7 cm, which can push or pull the wire with a force up to about 11 N. A schematic of the Model III source driver is shown in Fig. 10.1. The driver uses two small motors to direct the wire source into the calorimeter. One motor controls the source tube selection via a spiral indexer which can select one of up to 380 different channels, and the other motor drives the storage reel to extend or retract the wire, which travels in 3.2 mm OD low-friction acetyl plastic tubing to the calorimeter. Inside the calorimeter, the source wire travels in thinwall stainless steel hypodermic tubing of 1.3 mm OD and 0.97 mm ID.

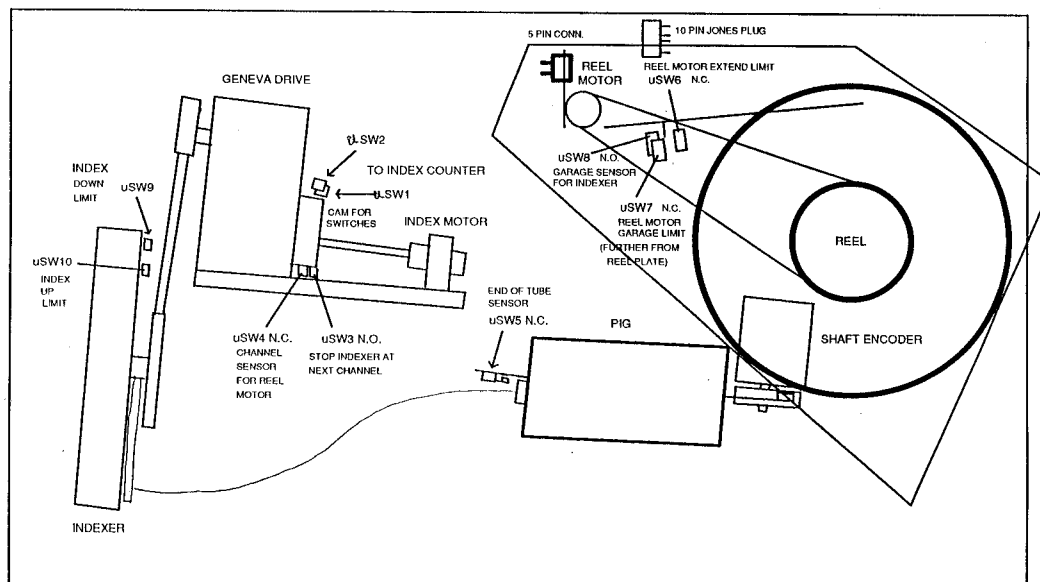


Fig. 10. 1: Schematic of a wire source driver which uses a storage reel.

Typical wire speeds are 5 to 10 cm/sec using the CDF Model III source driver with reversible DC electric motors. The wire speed is switchable to about one-half of the above speed if desired inside the calorimeter. The wire position is read out with a least count of 0.1 mm, and the indexer location is read in counts of one unit per channel, by batch counters which can be remotely interrogated and which also have visual readouts. The wire driver is controllable either by panel switches located on the electrical control box, or by a computer. The control box will be located within about 3 m of the computer, but can be located over 100 m away from the source driver.

The Model III source driver design used for CDF and for SDC, and proposed for most uses at CMS, has been described above. The design for the permanently installed drivers has two major changes: (1) to fit into the space at the back of a wedge, the indexer will be linear and will have fewer selectable channels (48 channels), and the wire driver motor and other elements will be confined to a maximum height of 7.5 cm, and (2) piezoelectrically switched "oil-free" air motors will be used, to permit operation at 4 T. The motors are made by the E2 Corporation, Model LZB 22 LR, and are readily available. The time between field servicings of these motors is claimed by the manufacturers to be approximately 1500 hours. Extensive tests of these motors will be done to determine the actual useful running time before maintenance is required. One calibration run into one scintillator layer in six HB wedges, at approximately five minutes per channel into 24 source tubes, would require two hours of running, and another two hours to monitor a second HCAL depth compartment.

A design using pinch rollers has been prototyped (Figs. 10.2 and 10.3) and is presently undergoing extended multi-cycle "torture testing". The pinch roller design is also well-suited to a slimline layout, although the prototype shown makes use of many Model III parts and is not yet arranged compactly. The pinch roller design, by almost everywhere confining the wire to a tube, eliminates the possibility of the wire's buckling, and also permits pushing the wire with more than 11 N of force if needed. However, it is believed that the reel drive, with 11 N of

force, would be sufficient for the proposed tube layouts; the recently-found low-friction acetyl tubing is very helpful in reducing the overall friction on the source wire.

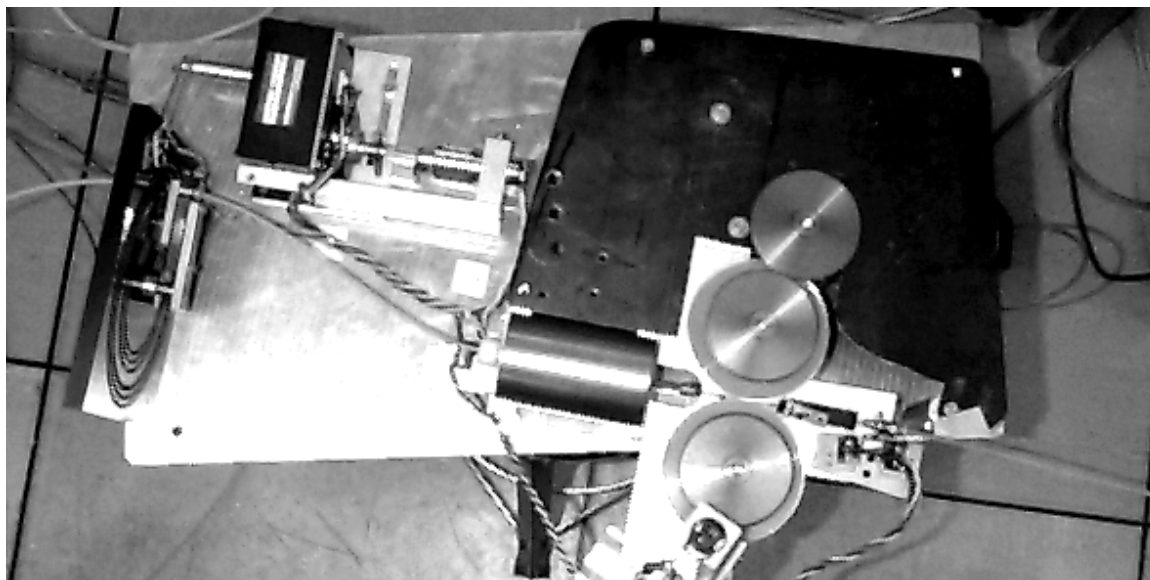


Fig. 10. 2: Top view of prototype pinch-roller variant of a wire source driver. The layout is not yet optimised.

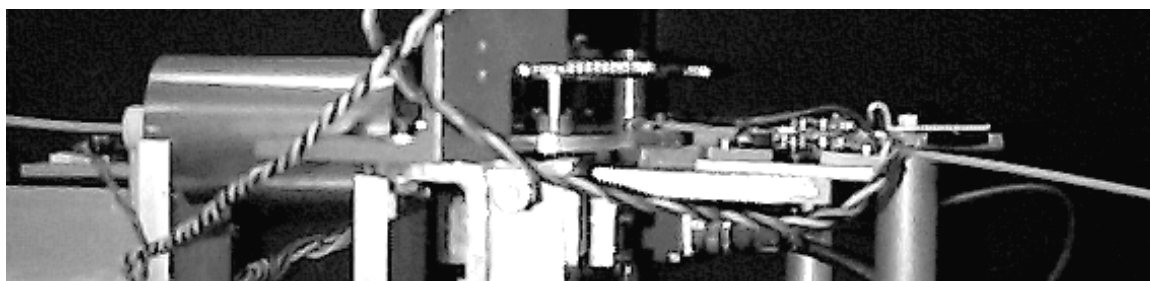


Fig. 10. 3: Side view of the prototype pinch-roller wire source driver.

The choice of permanently-accessible source tubes to only two layers of each HB tower and most HE towers is a compromise. There may be room for a longer linear indexer, or a modified indexer design, which could accommodate more than the planned numbers of source tube channels. We will investigate whether the number of index channels can be cheaply and easily increased. A few more permanently-accessible layers would provide more complete initial field-on sampling of the calorimeter, better redundancy of source access to the towers, and more complete sampling of radiation damage whenever desired. The extra cost and labor of installing more plastic tubes to the indexer is not large, since every pan-edge coupler will at least receive a short plastic tube. Because the air motor lifetime between servicings is not yet proven, extra permanent tubes might be used rather infrequently, but could provide useful options. Open access fingerprinting would still be by the Model III source drivers which use small electric motors.

Quality control

Source drivers of the final design for permanent installation will be extensively tested through many wire insertion cycles into a mock-up of the calorimeter tube layout. One such source driver will be exercised on the Pre-Production Prototype wedge, first at Fermilab and

later at testbeams at CERN.

Tube couplings will be installed under strict protocols, and the security and integrity of the couplings will be double-checked after installation. All source channels in the assembled calorimeter will be probed with a dummy source wire to check that their full length is accessible. (As discussed in chapter six, similar checks will be made on individual megatiles at production time.)

10.3.2 Layout

The layout of the source tubes is discussed in part in the Optical Systems chapter six. The metal source tubes run the full length of the megatiles, crossing near the centres of tiles except at the end of the megatiles, where the tubes make an S-bend to exit the pan as close as possible to the optical connectors. The bend radii are kept as gentle as possible to minimise friction and to minimise flexing of the source wire. The S-bend radii of the present design are 12 cm and 20 cm. Fig. 10.4 shows a plan view of a megatiles with source tube routing.

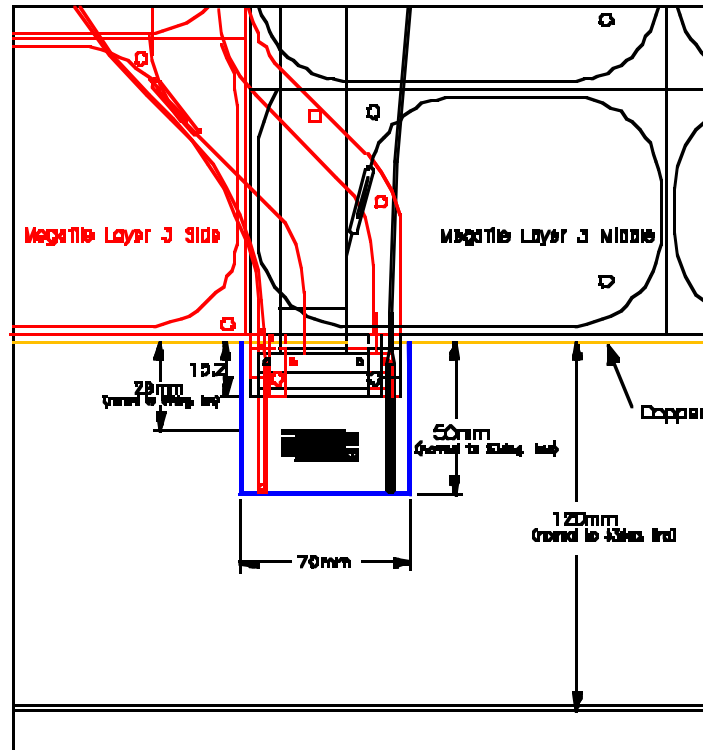


Fig. 10.4: Top view of the megatiles and connector layout.

At the pan edge, a brass transition coupler locks onto the metal tube with a 2-56 nylon-tipped set screw, and locks onto the 3 mm (1/8") diameter acetyl tubing with a paraxial 3-48 screw whose threads bite into the plastic. A cone of 18.5° full angle guides the tip of the wire into the narrower metal tube. Both the optical couplers and the source tube couplers protrude a short distance, (of order 1.8 cm beyond the edge of the megatiles, or 1.5 cm beyond the copper, for the source tube couplers), into the protected channel dedicated to them. Front and side views of the couplers are shown in Fig. 10.5, Fig. 10.6 and Fig. 10.7. A more panoramic view of the end of a wedge, showing the dedicated channels and source driver, is in Fig. 10.8. One source driver, with a 35-foot (10.6 m) source wire can access up to 7 wedges.

10. CALIBRATION

For symmetry, both HB and HE will use one source driver per 6 wedges (or per 120 degrees in azimuth).

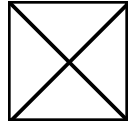


Fig. 10. 5: End view of HB megatile-edge source tube coupler.

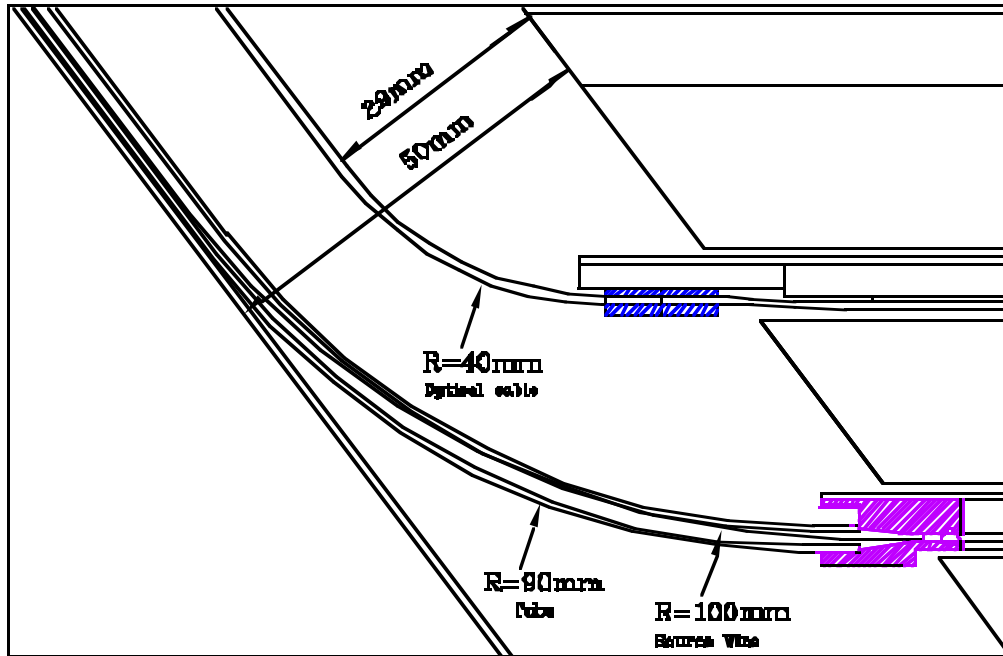


Fig. 10. 6: Side view of the edge of an HB megatile showing the source tube coupler and the direct R-Z bend of a permanent plastic source tube.

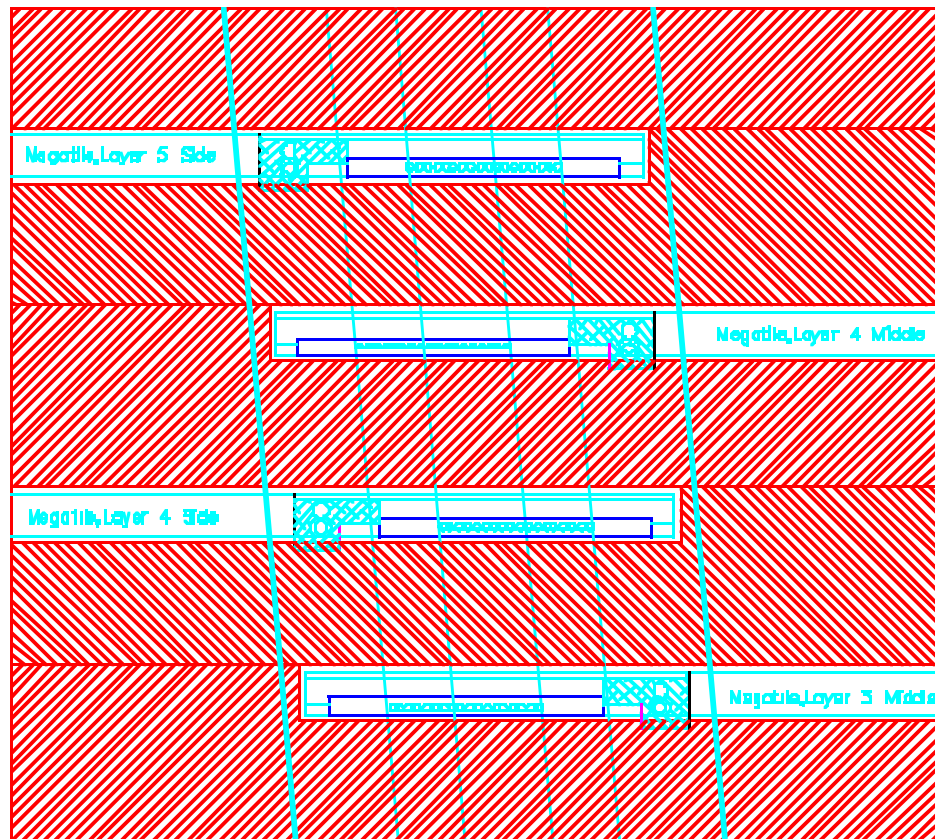


Fig. 10. 7: End view of HB megatile optical and source tube couplers.

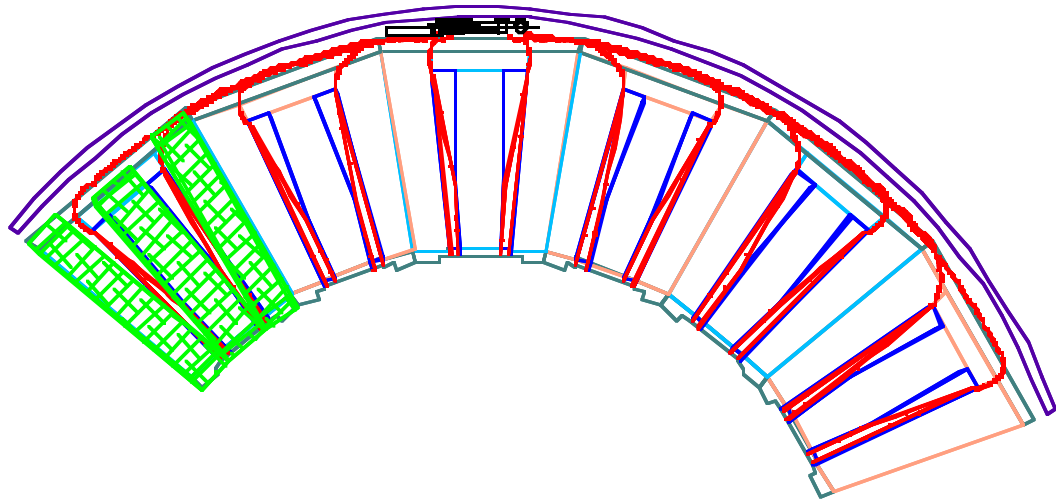


Fig. 10. 8(C.S.): Panoramic view of the end of six HB wedges, showing the channels dedicated to the optical cables and source tubes, source tube routing, and a slimline source driver. The leftmost wedge also indicates (hatched) a possible routing of the overlying services from HE and Tracking.

Most of the layers will be coupled to a source driver only on occasions when the endcaps are retracted. For HB, if the innermost 40 cm of the channel is buried under other services, the plastic tubes will be conducted out beyond a radius where the overlying services have fanned out away from covering the HCAL channel. A possible routing of the overlying services is

10. CALIBRATION

shown hatched in the leftmost HB wedge in Fig. 10. 9. As soon as possible towards the back of the wedge, the HCAL channel height should increase to more than 5 cm above the copper, to ease the wire bending radius when entering the outer calorimeter layers.

All plastic tubes will be permanently attached to the couplers at the edge of the megatile. Quick-release barrel connectors will be used occasionally to couple, via 3 mm (1/8") plastic tubing, a roving source driver to all of the source tubes in a tower, to repeat the "fingerprinting".

One layer of tiles in each depth compartment will have light injection fibres and will also have source tubes coupled via plastic tubing to permanently-installed source drivers. The plastic tubes will run from the pan edge to the back of each wedge, in the HB channels shown in Fig. 10.8. The tubes turn and run azimuthally just inside the cryostat towards the source driver. One slimline source driver will serve 6 wedges. A radial view of the driver and associated plastic source tube routing is shown in Fig. 10. 10.

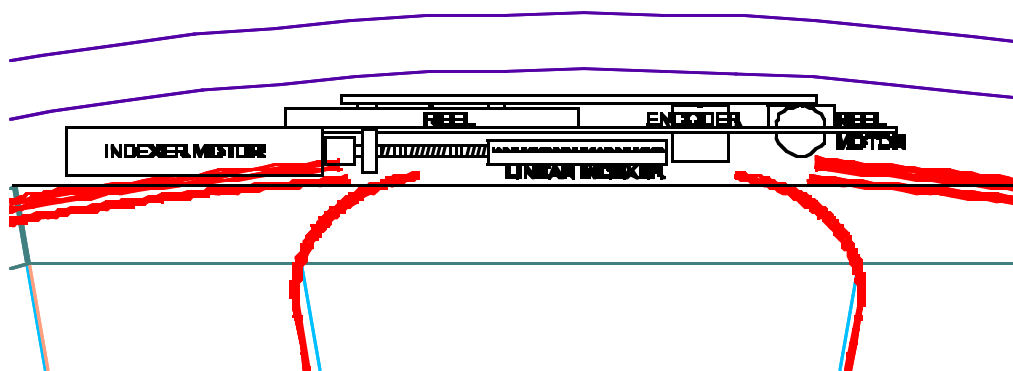


Fig. 10. 9: Z-view of a slimline source driver. For clarity, the 90° bends of the plastic tubes into the Z-direction are not shown.

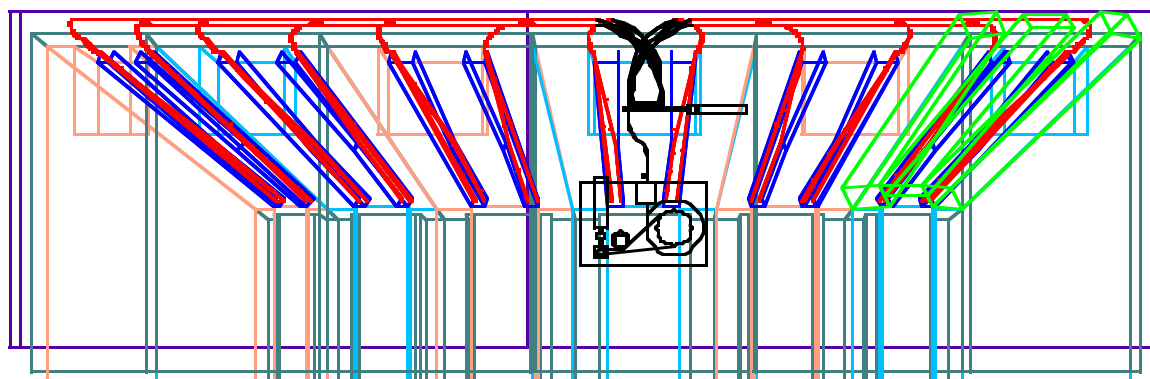


Fig. 10. 10: Plan- or R-overview of source tubes and slimline source 4,5,5,6, driver at the back of an HB wedge.

Each driver will require a 90 psi air supply, with one air hose per half-barrel, and one hose per endcap, coming from outside the detector. Each installed driver will require a separate multi-wire cable running to its electrical control box located in one of the control rooms in the cavern wall or at the surface.

For HE, the space constraints in the 12-cm crack are quite different: the source tube routing is not constrained to narrow phi intervals, but on the other hand less space may be

available above the metal calorimeter plates. The solution is to bring out the source tubes at the edge of the megatile pointing in the phi direction, via a 90° bend. At that point, quick-disconnect CDF-style transition couplers are installed on the ends of the metal source tubes and mounted securely to the edge of the megatile. These couplers are specially modified brass Parker fittings, with a steep internal cone leading to a socket for the steel source tube. The steel tube is permanently locked in with a 2-56 nylon-tipped set screw. Occasional-access sourcing by roving source drivers is via the 1/8" plastic tubing into these quick-disconnect couplers. Permanent plastic source tubes routed to selected tile layers will couple into the same type of quick-disconnect couplers. These permanent plastic tubes will make 90° turns to run generally in the Z direction to the rear of the calorimeter and then turn toward the source driver.

10.3.3 System interfaces

The primary source driver system interface is: (1) at the front panel of the electrical control box, via a 25-pin D connector to the TTL digital logic expansion card in the PC. The traffic consists of motor control signals and status signals; (2) the RS485 interface between the two batch counters (wire position and index channel counts) and a serial Communications port.

The control computer contains software to control the motion of the source wire and the selection of channels. The PC will communicate with the host computer which does the run-control and the DC source current data acquisition from the HPDs.

10.3.4 Data acquisition and processing

During source calibration operations, the calorimeter readout system will be operated in its normal mode at the normal clock speed with the calibration established through extreme oversampling. For the case of a 10 cm tile and a source speed of 5 cm/sec, averaging data samples over 10 msec intervals provides 200 data points across the surface of the tile. Since the majority of the source data will be acquired before installation in the cavern or at times when the CMS TriDAS system is not expected to be operational, the Detector Control System (DCS) has been selected to acquire and process the data. This system also provides control, display and database services for the calibration process and acquires the source position readings needed for the calibration algorithm.

Each readout crate in the system contains a DCS processor. During source runs, this processor becomes the master and the crate is disconnected from the normal data path to the farm. The trigger and data acquisition cards continuously receive the data stream from the front end digitizers into the first-level trigger pipelines. A first-level trigger accept, generated by the DCS processor, causes 8 groups of 16 consecutive readings to be moved into the derandomizing buffers. Subsequently, each group of 16 is sent through the second level filter which performs a sum operation. Finally the 8 summed results are readout over the VME bus into the DCS processor for further averaging and histogramming. Only those channels for the set of tiles in the calorimeter layer being scanned are read out, but all of them (up to 34 for the longest tile tray in the barrel) are readout for each first-level yes independent of the source position.

Finally, the processor executes the calibration algorithm on the histograms for each tile. Since the number of photoelectrons expected in each measurement interval is small, the calibration amounts to fitting the data to a Poisson photoelectron distribution convoluted with a Gaussian noise distribution and extracting the average number of photoelectrons per measurement interval. The measured spectra are available to the operator at any time during the

10. CALIBRATION

run and particularly at the end for diagnostics if the algorithm reports a calibration failure. There are 14 source systems in total, and using crate based processors allows for parallel operations without a rate penalty.

10.3.5 Access, maintenance and operations

The initial fingerprinting and calibration will require access to the "occasional-access" source tubes with the detector open, and also requires measuring the source response of selected scintillator layers with the magnetic field on.

Subsequent monitoring by the moving source, of gains and of light injection to the special layers, can be done as often as desired. It is envisioned to take place at one to two month intervals, or as dictated by our experience with the stability of the light injection monitoring and of the various light injection paths to HPDs and to individual tiles.

Access to the source drivers and their associated tube manifolds will be only when the endcaps are retracted, which is expected to be at very infrequent intervals of perhaps one year. Access to the installed source drivers, for possible maintenance, must be feasible. This is an important integration issue involving the pipes and cables which run in the crack between HB and HE and then along the inside of the magnet cryostat.

10.4 LASER CALIBRATION AND OTHER LIGHT INJECTION

The HCAL calorimetry systems necessitate a precise calibration scheme. Calibration systems are needed to:

- a) Monitor the performance of PMTs and front-end electronics, for each channel (laser)
- b) Maintain calibrations from a test beam or collider data. Both absolute and tower to tower gains need to be tracked in time.
- c) Set timing offsets for each channel

Monitoring of the system has to be far more frequent than the in "in situ" absolute calibration with collider data. Monitoring will be accomplished with the help of well-controlled light sources (laser and blue LEDs) which will be externally generated and distributed throughout the system. The light injection can be done several times per day (during nonfunctioning of the collider). These systems will be used for photodetector gain and linearity monitoring and for radiation damage monitoring. In principle the light injection response data can be made available very quickly to an operator to check the performance of all the calorimeter channels. A number of quartz and plastic-scintillator-tile hadronic calorimeter prototypes were monitored during the 1995/1996 test runs using various combination of LED and laser systems. Our data indicate that these systems can deliver monitoring of photodetectors better than 3% under realistic experimental conditions. We expect that with further optimisation, this precision could be improved to 1% which is adequate for HCAL systems.[9]

10.4.1 Specifications

DYE LASER: A pulsed nitrogen dye-laser can be tuned both in wavelength (337-500 nm) and intensity (neutral density filters) remotely for multiple purposes. At a few Hertz repetition rate, a commercially available pulsed N₂ laser with 4 mJ energy at 337 nm can provide 225 μ J if a dye is used. This corresponds to 5×10^{14} photons at 450 nm. If we assume that one million p.e. per channel are needed for monitoring and that a conservative estimate of quantum efficiency, light losses at splitters and connectors is made, then we need about 3×10^{12} photons

per one side of HF, for example. The dye has the virtue that a tuneable frequency light source is possible over a range of 350-500 nm. The tuning requires about 1 second to reach any given wavelength. The manufacturers indicate that a command jitter of less than 1 ns is possible with modest development. In test beam work, we have experience with sealed (open TEA) nitrogen pulsed lasers which provided 3 ns (0.6 ns) wide pulses.

LED: LEDs serve as an additional information source, namely: to extract a gain and single photoelectron level via the statistical method. LEDs are also logistically useful at times or places where the laser is unavailable, such as in the HO-B and HO-E.

- Superbright blue LEDs based on GaN grown on SiC substrates are newly available in the market. We have already used these LEDs in the test runs.
- The typical brightness for these LEDs is now about 1000 mcd.
- They have a remarkably low dependence on temperature, due the large direct bandgap in GaN.

10.4.2 Design

LASER: A 4 mJ laser will be suitable for the purpose of monitoring HB, HE and HF simultaneously. This laser will be housed in the counting room.

In the test beam work, we have used a sealed nitrogen pulsed laser which provided a 3 ns wide pulse at frequencies from 1 to 20 Hz. Each pulse was about 120 μ J at the nitrogen wavelength of 337 nm with a 5% variation in power from one pulse to the next. The beam size at the exit of the laser cavity was 3 mm by 8 mm and the beam divergence was 5 mrad by 8 mrad. This laser can be externally triggered with a minimum of 1 μ s wide TTL pulse. Our present system and related optics are shown in Fig. 10. 11 through Fig. 10. 14. The system contains vertical and horizontal slits which reduce the intensity of the light in x and y directions respectively. There are 4 beam splitters that reflect some small fraction of the light to the photodiodes and the transmitted light is captured by a 1 mm inner diameter quartz fibre.

10. CALIBRATION

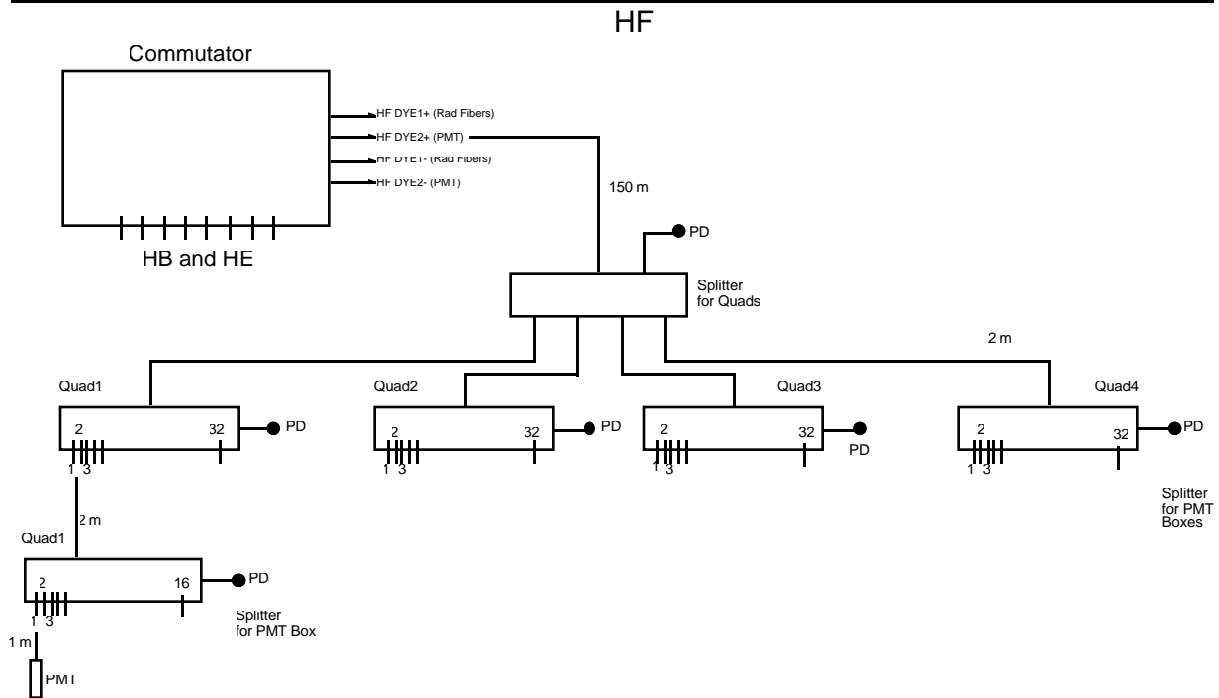
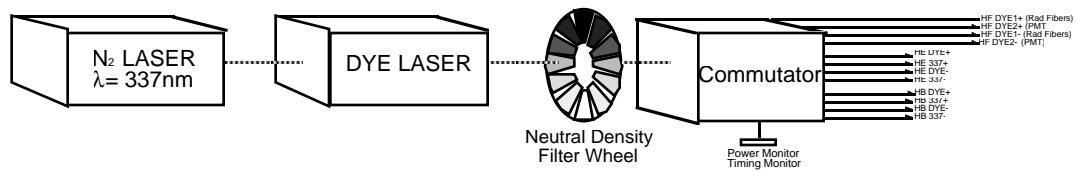


Fig. 10. 11: The layout of the HF laser light distribution system. The HB, HE system is shown in chapter 7.

CMS HCAL Calibration and Monitoring Laser System

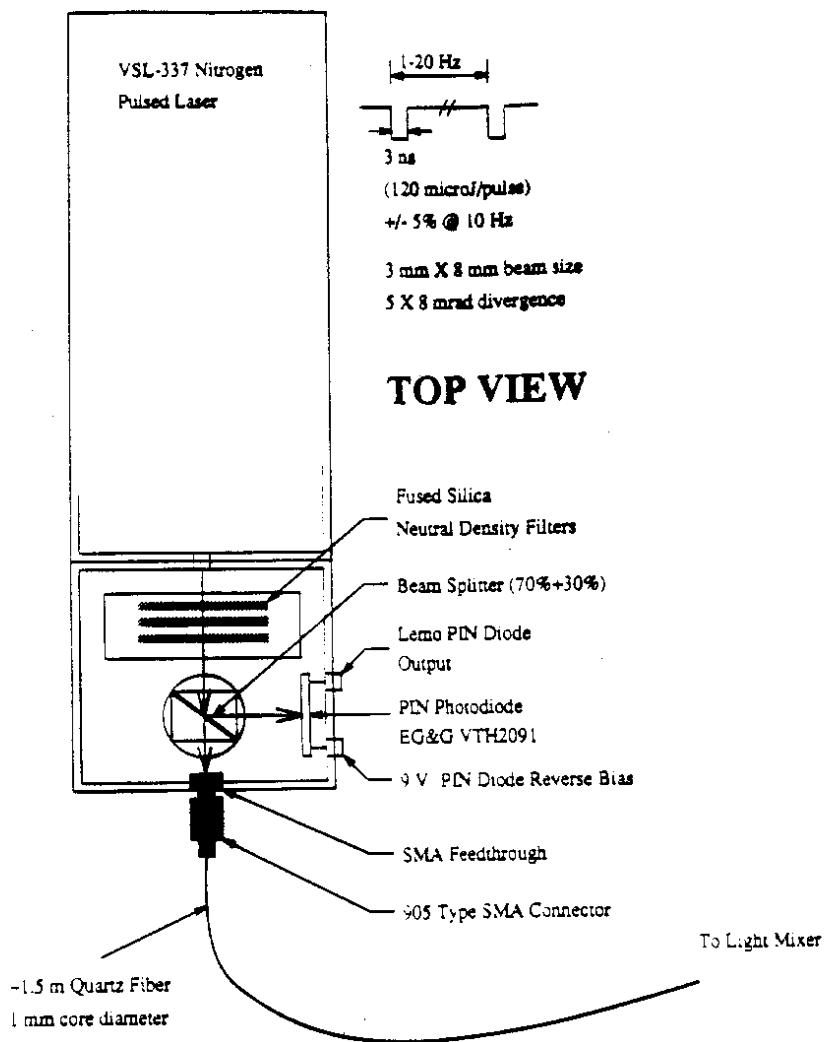


Fig. 10. 12: Laser light injection system and related optics. The box attached to the laser source houses necessary components for pulse-to-pulse monitoring of the laser.

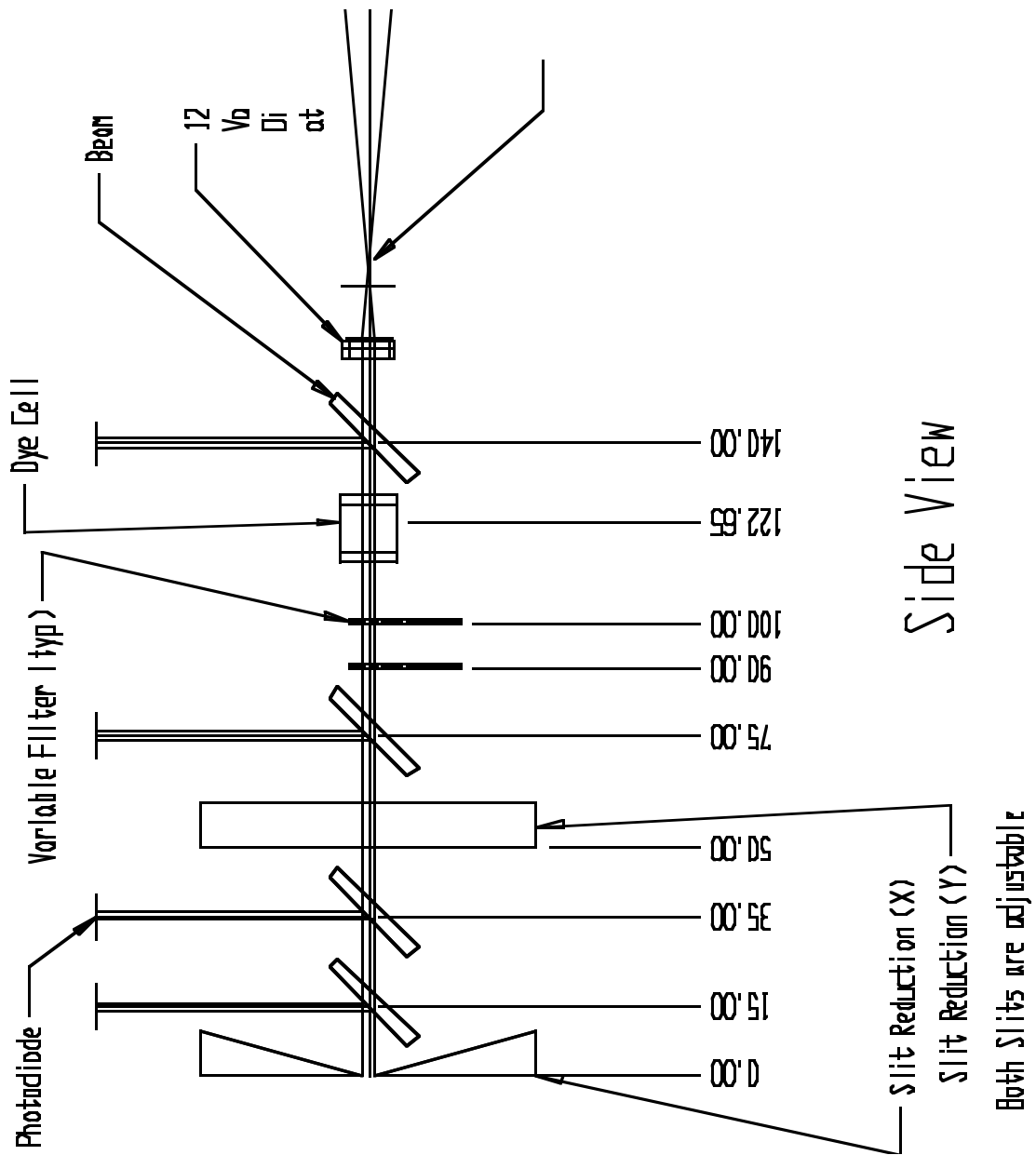


Fig. 10. 13: Laser light injection system and related optics.

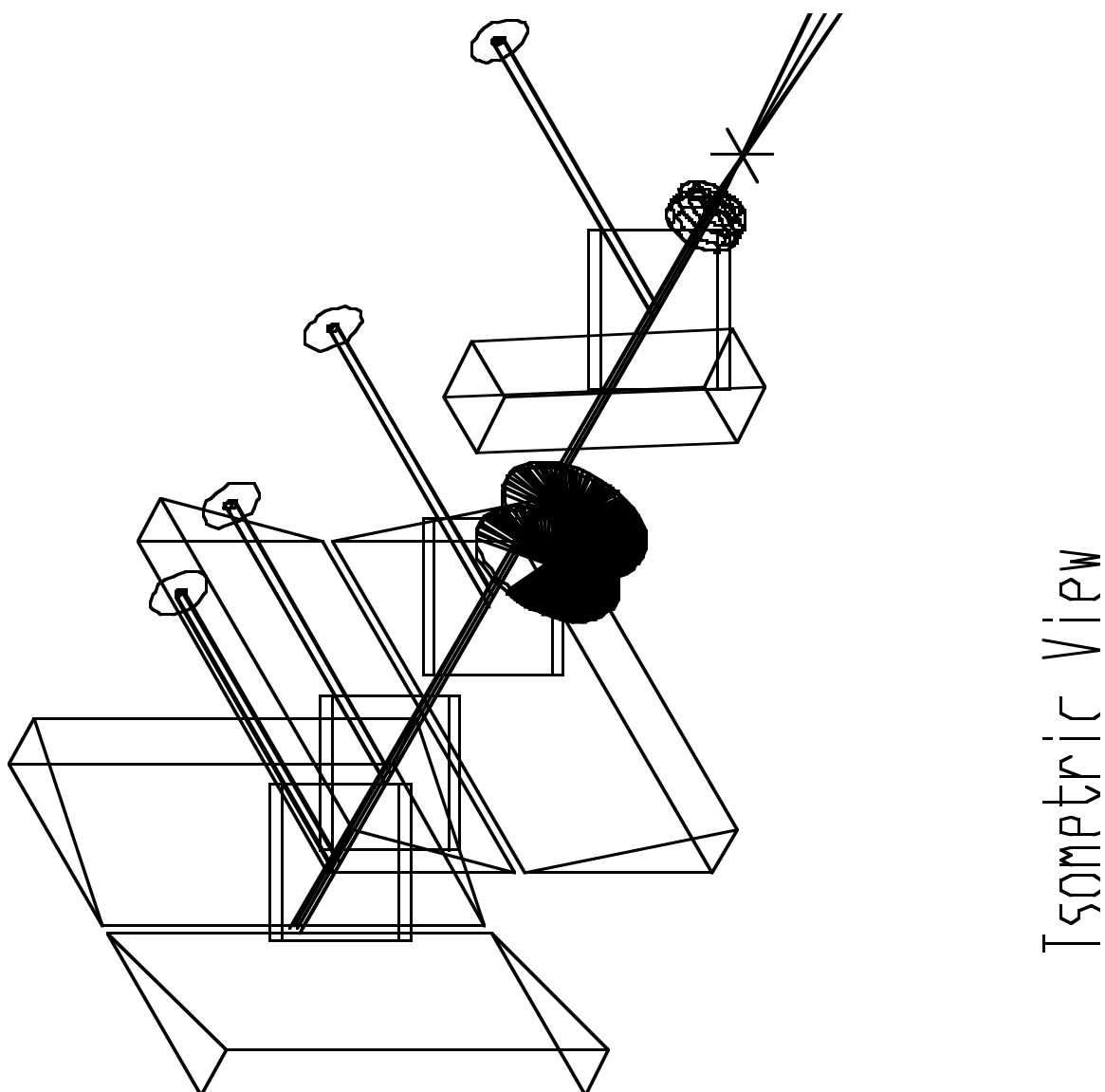


Fig. 10. 14: Isometric view of laser light injection system.

The system would have the nitrogen laser triggered by a programmable module. The laser light pulse is split, part of the light is fed to a PIN diode to control the pulse amplitude (about 10^6 photons to avoid the use of an amplifier). The other part of the light is fed to a filter wheel to change the light intensity in steps to cover four orders of magnitude (about eight steps) to control the dynamical range of photodetectors and ADC. The position of the wheel is controlled by a programmable module. The programmable module allows the introduction of a fixed delay between the laser trigger and the ADC gate (with few ns step) to measure pulse position within the gate for each channel.

Quality control

For the HB, HE and HO we will build a LED system (blue LEDs) into the decoder box to be used in stand-alone mode. We also have an independent LED system for the HF. This HF LED system is foreseen to be used for tuning the readout chain (PMTs, FERMI Boards, cables, connectors) and for setting/monitoring the PMT gains. We propose to use blue LEDs. In this system, we will have a VME controller for the LED drivers. The LEDs will be connected to

10. CALIBRATION

bundles of short fibres with 100 micron diameter and each fibre is connected to a particular PMT. A LED driver has four channels (one channel per LED). There are 20-30 fibres in a bundle and 5-10 LED drivers will be sufficient for one half of each HF calorimeter. The LED driver scheme is shown in Fig. 10. 15. Fig. 10. 16 shows the complete LED test system.

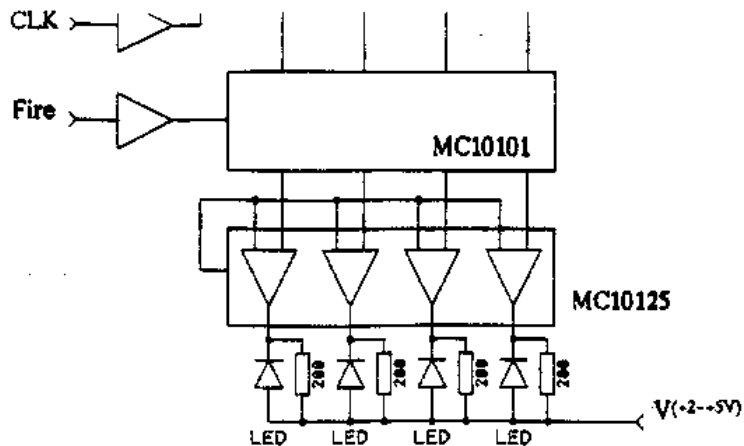


Fig. 10. 15: LED driver scheme.

Stability of quartz fibres is an important issue for small angle tiles. A measurement of the radiation hardness of the quartz fibres shown that there are available fibres which can satisfy the required measurement precision without degradation up to 50 kGy (5 Mrad).

A second reference monitor, for redundancy, consists of a CDF-style temperature-stabilised PMT which simultaneously views one of the fibres and an ^{241}Am -loaded NaI scintillator. The stability of the PMT response is monitored using the 5.4 MeV ^{241}Am alpha particle peak. The temperature dependence of the NaI response, $\sim 0.2\%/K$, requires controlling the temperature of the PMT and the NaI to better than about 3 K. Use of this reference phototube is contingent upon being able to locate it in a sufficiently magnetic-field-free region, with suitable magnetic shielding.

A third reference monitor is an HPD which views a light-injection fibre as well as a temperature-stabilised scintillator tile which can quickly be exposed to a small dedicated ^{137}Cs source. This monitor would be installed outside the calorimeter and probably close to the laser/LED light source. A somewhat similar system, but with a manually-moved ^{137}Cs wand source, was used at the H2 testbeam in the summer of 1996.

LED TEST SYSTEM

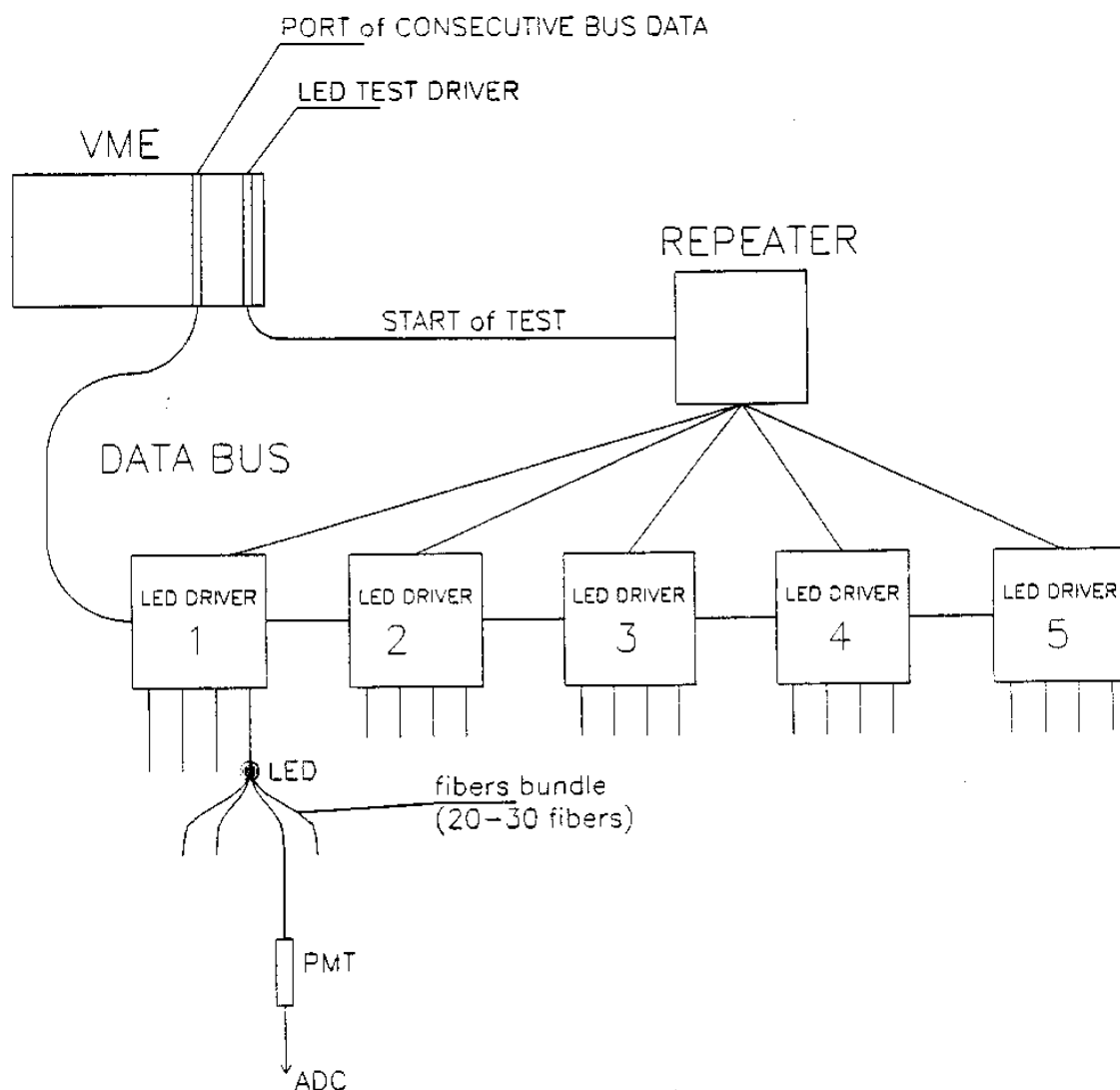


Fig. 10. 16: LED system.

10.4.3 Layout for HB, HE, HO and HF

The single laser light system uses quartz fibres, where the diameter starts with 1 mm and after all the splits ends up with 200 micron quartz fibres. First, the laser pulse passes through a filter wheel where the intensity can be varied by four orders of magnitude. Next the light is sent to a commutator that can send the light to any one of 12 outgoing fibres. These are as follows: four to HB, four to HE and four to HF. The HB fibres are routed as follows: 2 to each side, one of each side for the decoder boxes and the other to the scintillator layers. The light splitting is as follows. The decoder box fibre is split 18 ways, one for each decoder box. Inside each decoder box, it is split again so each pixel of every photo detector gets a 200 micron fibre. At this split the blue LED is also attached to the splitter so a light signal from the LED can use the same fibres to illuminate the photo detector pixels. The other fibre for the scintillator is also split

10. CALIBRATION

18 ways, one for each wedge. For each wedge, each fibre is again split 8 ways, where four fibres each are connected to the two tile layers that have the laser system. Each tile layer receives 2 fibres for the central megatile and one each to the edge megatiles. At the tile trays, the light is fanned out from the input fibre through a small mixer to the 16 tiles by 200 micron quartz fibres.

The HE fibre divisions are very similar to HB, except that there are 12 wedges instead of 18[10]. The HF is also similar where one fibre on each side is split 4 times, one for each quadrant and split again 32 times, one for each photo detector. The other fibre on each side is used to determine radiation damage by routing the light through a fibre near maximum irradiation as explained in more detail below.

The HOB and HOE only have blue LED in each decoder box, where plastic fibres send this light to each photo detector. Since HO will see very little radiation damage, plastic fibres are sufficient.

For the HF, we are also considering a design with a separate laser and LED calibration and monitoring system to provide an alternative system which could be more suitable for the needs of HF, and would simplify the logistics of monitoring HF quartz fibre radiation damage while the other laser does the routine monitoring of HB and HE. The laser system for the HF is very similar to the one used in the central calibration system, namely a pulsed nitrogen laser with trigger system, selectable colours, wide dynamic range intensity filter wheel with reference PIN diode for intensity monitoring and timing. Another reason why we might need an independent laser system for the HF is to monitor the radiation damage to the quartz fibres. In this radiation damage monitor, a number of fibres from the distribution system will traverse the entire length of each tower and return back to the photodetector. In this system the laser and attenuator are connected through a 300 micron diameter quartz fibre which is about 10 m long. The function of the attenuator is to change the intensity of the light output over a wide range (100) by changing the distance between input and output fibres. The diameter of the output fibre is 1 mm and it is about 15 m long. Both fibres going into the attenuator are matted. The output fibre is then put into a distribution system which is 0.5 m long fibre of 2 mm diameter. This distribution system has 20-25 fibres of 130 micron diameter. These 130 micron fibres are then distributed to the calorimeter tower bundles and light guides

10.4.4 HF normalisation

In HF, the absolute and relative tower-to-tower calibration will have to come from the collider data as di-jet E_t balancing and photon-jet E_t balancing. Monte-Carlo studies of Z +jet events as a function of missing E_t indicate that the necessary calibration precision is 5%. The HF can be calibrated using the entire sample of di-jet events. By requiring one jet detected in the HF and the other in another part of the calorimeter system (HB/HE), the intercalibration between these systems can be verified by E_t balancing. Similarly, gamma-jet events can be used for calibration using E_t balance but in this case a single photon real energy measurement is necessary from the ECAL. There are other possibilities and these are also under study. For example there are low cross section processes that possess jets of well understood energy, a high P_t Z recoiling off of a single jet. The high energy and luminosity of the LHC may supply enough of these events for quantities useful for calibration. Another interesting process is $t\bar{t}$ production. Here both top quarks decay into $W+b$. If one requires one W to decay leptonically, this provides our trigger. The other W decays into quarks that form jets. These two jets, which will reconstruct to the W mass, provides our means of calibration. To eliminate the

combinatorial confusion, we require that both b s are tagged by the tracker.

10.4.5 HF radiation damage monitoring

Radiation damage affects light transmission in quartz fibres mostly below 425 nm and above 460 nm. The possibility of tuning the laser to various frequencies provides a handle to monitor radiation damage to fibres. For this purpose, we will have fibres that traverse and then return the entire length of the calorimeter modules for each tower. In order to monitor the photodetectors, light from the source will be split and cascaded to the PMTs with quartz fibres. With similar systems, long term stability of 1.4% was achieved in large experiments over a few years.

10.4.6 Other HF normalisation

We recently started investigating the possibility of using a moving gamma or beta source system similar to the gamma source system that will be used in the HB and HE systems. If sufficient light is generated in the quartz fibres, this could provide a useful cross-calibration of HF towers, as well as providing a standard illumination to check the light injection monitoring of photodetectors and of individual tiles. A 0.9 mCi ^{90}Sr beta source inside a standard 18 gauge source tube next to the same four quartz fibres gave a DC current of roughly 15 pA. Stronger ^{90}Sr wire sources will be difficult to obtain, and the radiation is probably too local. ^{60}Co gamma radiation, much of which is above 1 MeV, will be investigated soon, and is expected to excite the quartz fibres efficiently via Compton electrons which are above the Cherenkov radiation threshold in quartz. This radiation will also penetrate the copper calorimeter matrix to illuminate a greater volume of quartz fibres.

As another method of normalisation, the long term response of each calorimeter channel can be monitored using energy flow. This can be achieved by measuring the photodetector dc-current as a function of luminosity. The dc-current will be integrated with a few microsecond integration time and this functionality will be designed into the front-end electronics, and is also necessary for source calibrations. As a function of η , we expect to monitor relative calibration and to detect nonuniformities in the detector when normalised with the luminosity at CMS.

10.4.7 Data acquisition and processing

During light injection operations, a large number of channels are illuminated. Readout requirements range from the full system of about 16,000 channels to one of six possible partitions corresponding to the two halves of the HB, HE and HF detectors where 2,000 to 3,500 channels are involved. Because of the volume of data and the need to cover the full dynamic range during a calibration, the normal TriDAS system has been selected for data acquisition and processing. The exact division of control and data archiving functions between the on-line processor farm and the DCS general purpose computing services has yet to be determined.

Pulsing of the laser or the LED's is controlled by presetting a counter on the 40 MHz system clock. For the LEDs, this counter is in the channel control chips for the front ends; for the laser, the counter is incorporated into the laser controls. The front end digitizers operate in the normal mode at the normal clock rate and send a continuous data stream to the first-level trigger pipelines. A first-level trigger accept is generated with the proper timing and distributed to all channels through the normal Timing and Trigger Control mechanism. An automatic second-level trigger accept then causes the data to move through the derandomizing buffers into

10. CALIBRATION

the second level filter which extracts the total signal from the time frame and places the result into the readout FIFO. The full block of data, 2,000 to 16,000 channels, is then moved into the farm for processing.

Readout of the HCAL is done through 16 Front End Drivers each capable of 200 Mbytes/sec. For the case of the whole detector, the maximum event rate is then 100 kHz. Data processing in the farm, initially to accumulate the histograms and then to extract the mean and sigma and prepare for the next point, will certainly reduce the event rate. Taking a one-to one correspondence between farm nodes and readout drivers gives a work load of 1000 channels per processor. Allowing for 10 operations per data word in a 200 MHz farm processor gives an event rate of 20 kHz. For the case of 8 ranges (chapter 9.3), 5 different points on each range, and 10,000 events per data point, the complete calibration could be done in 20 seconds.

Sixteen calibration constants are determined for each channel, a slope and an intercept for each of the eight ranges. This 512 Kbytes is to be archived through a bridge to the DCS database services. At the beginning of a run, downloading of the calibrations into the readout lookup tables can be accomplished either through the DCS path to the front end crates or through the bridge to the farm and the data acquisition system path.

Usage of the 3.17 microsecond gap in the machine fill is problematic at this time. The time needed to switch from physics data to calibration mode, take one light flasher event, histogram the results, and switch back to physics data mode is poorly known and estimates have a large uncertainty. Also, the stability of the calorimeter system is expected to be such that calibrations are only needed between fills of the collider, once or twice per day. On the other hand, it is possible that unexpected luminosity-dependent effects may require that calibrations be taken during a store. Thus, development of the relevant systems will be followed until a definitive answer can be established as to the viability of interleaved data and calibration operations.

10.4.8 HF calibration and monitoring

In the following, we describe the hardware calibration and monitoring system for the HF.

Hardware tools of calibration and monitoring of HF

The calibration of individual towers directly affects the overall energy scale of the HF and the effective energy resolution at high energies due to the internal tower-to-tower calibration uncertainties. The requirement on the HF resolution implies that the calibration uncertainty for tower-to-tower response of $\sim 3\%$ and on the overall energy scale uncertainty of $\sim 3\%$ are acceptable.

The hardware system for the calibration and monitoring should address the following:

- light response of the quartz fibres in a high radiation environment and the efficiency of a light collection system
- the light signal amplification (PMT gain)
- the performance of the entire chain of front-end and read-out electronics

As the HF calorimeter systems will have to function in a severe radiation environment, one should take special care as to the reliability of the hardware monitoring system and should build in redundancy and flexibility into its components. The control and monitoring of the above ingredients will be realised by the following hardware and procedures :

- quality control of the technology at the mass production stage

- beam tests
- calibration *in-situ*, using physics event signatures
- light emitting diode (LED) monitoring system
- laser gain monitoring system charge injectors for noise, gain, non-linearity monitoring and for timing adjustments of the chain from PMTs to the front-end electronics.

Quality control at fabrication

Control at various stages of mass production is necessary in order to ascertain adherence to the optical and mechanical specifications. Here, we foresee:

- an effective procedure for the identification of possible assembly faults in the calorimeter towers;
- incoming control of both optical and mechanical properties of quartz fibres - the homogeneity of the active media in individual towers have to be kept at the level of $\sim 1\%$;
- control of mechanical tolerances of the copper-quartz fibre matrix - here we keep the copper-to-quartz volume ratio at the level specified.

Beam tests

The test beam runs serve as the final step of the mass production and as the first estimate of light yield. The following points should be addressed:

- uniformity of the tower responses;
- response to electrons and corresponding light yield, $N_{p,e}/\text{GeV}$ per tower;
- intercalibration of tower-to-tower;
- response to hadrons;
- a first approximation to the calorimeter absolute energy scale.

We are investigating the use of moving Cobalt ^{60}Co photon sources to link test beam calibrations to the installed calorimeter in the collision hall.

Physical Calibrations

The next iteration of a calibration after the beam tests are the analysis of the LHC data samples taken *in-situ* using select event signatures. Such methods afford us calibration of the light yield of every tower and equalization of the relative responses of towers. These changes are expected come from:

- radiation damage - the most dominant factor;
- aging of quartz fibres;
- deterioration of various optical contacts;
- other similar effects.

The nice possibility for a calibration of long term changes is provided by the recent study of the energy spectra of the minimum bias events. The requirement of the similar slopes for the energy deposited in individual towers constrains the relative tower-to-tower calibration factors. The final calibration of the overall scale will exploit several physical processes and will rely on the redundancy of the CMS detector. Among the possible candidates are two-jet events with one jet to be detected in other CMS calorimeters and the second one in the HF with balanced transverse missing energy, and the QCD Compton process with the photon to be measured with ECAL and the balancing hadron jet flowing to the HF section.

Laser Gain Monitor

The HF calorimeter employs the global laser system of CMS HCAL. This system enables us to simulate the light pulses similar to the ones that are generated in the HF in time, spectrum and amplitude characteristics. It serves for:

- linearity test of PMTs, front-end and read-out electronics chain in a wide dynamical range,
- fast signals for timing measurements and adjustments on channel-to-channel basis,
- the short term monitoring and the measurement of the PMT gains.

The principal scheme has been successfully tested with an HF prototype of during the 1996 test runs. The analysis of the data collected has proved the feasibility to reach good light injection uniformity, better than 5%. The pulse to pulse variation of laser light is monitored by a series of PIN photodiodes.

LED System

The monitoring redundancy for the HF calorimeter is a necessity since it is located in an extremely harsh radiation environment. The LED system not only provides a low cost redundant system but also brings a set of advantages. This system is:

- technically simpler and more versatile than the laser system,
- relatively inexpensive,
- stable and provides good pulse-to-pulse amplitude stability,
- easy to construct fast triggers, and
- easy to monitor using stable photodiodes.

We plan to use the fast and bright blue LEDs. The system will be used for:

- a number of tests during the assembly and installation period as a stand-alone tool,
- determination of PMT gains using the method of photo-electron-statistics and to equalise the gains; and we expect to reach the uncertainty of less than 3%,
- monitoring short term gain drifts of every tower.

The PMT gains can be checked and the HV adjusted during the short breaks in the collider. In addition, the timing properties and the behavior of the whole readout chain from PMTs up to the front-end electronics can be tested at high rates, 40 MHz. The LEDs can fire during the regular data taking and can be timed with empty bunches. This makes monitoring of short term gain variations and almost on-line correction of the data possible.

Laser monitoring of the quartz fibres

This system is a tool for monitoring of the long term radiation damage of quartz fibres. It exploits the same laser light pulser as laser calibration system. The light is injected to a control quartz fibres embedded in selected calorimeter towers. With the possibility to tune the laser wavelength, we will be able to measure the light attenuation as a function of wavelength in fibres due to the long term radiation damage.

Moving radioactive sources

We will investigate the use of ^{60}Co gamma sources in two systems:

- a) moving a collimated source across the front face of the calorimeter (x - y remotely controlled motion), and/or
- b) wire sources moving in longitudinal channels within the calorimeter.

The former system could provide tower-to-tower relative normalization and carry

testbeam calibrations to the collision hall. The motion of the radioactive source is accomplished by a remotely controlled x - y translator where the precision of motion is required to be within a millimeter in both horizontal and vertical directions. Two x - y motion devices are planned per HF side, each serving a half of the detector. The latter system could provide direct scans of the longitudinal distribution of radiation damage to the quartz fibres. Two remote controlled motors per HF side will service the selected source tubes that are embedded throughout the HF absorber. The necessary source strengths need to be determined. Very intense ^{60}Co sources carried inside the standard 0.7 mm diameter "wires" can be obtained, relatively inexpensively, from the North American Scientific Company, North Hollywood, CA. These investigations are important since we can transfer the calibration to each tower with the aid of a source as in the HB and HE systems. This will therefore eliminate the need of a test of each tower in the beam.

Charge injectors

The Q-injection system will be used for the noise, gain and non-linearity studies of the QIE5 structures to be used as charge sensitive ADCs for the calorimeter signal digitization and readout. We expect also that the system will provide us with the possibilities to trace the time properties of the front-end electronics.

10.5 OTHER SYSTEMS

It is assumed that the magnetic field will be mapped. Nonetheless, three-axis Hall probes should be installed in a variety of locations in HB and HE, especially to keep track of any residual magnetic fields when the magnet current is turned off, as well as to measure the full field. The reason is to provide a redundant way (in addition to field-on radioactive source calibration) to track the brightening of scintillator, which is quasi-logarithmic in the magnetic field. Thus, a field-on calibration could be based on bench-top measurements of the brightening curve, known starting and ending values of the magnetic field, and magnet-off source calibrations.

This system of Hall probes might be categorised along with other slow- controls items such as temperature probes, and read out like other environmental variables. However, it is anticipated that the Hall probe data will be needed only occasionally, mainly to provide field "on versus off" information. Hence a more primitive readout system could also be acceptable.

No explicit design exists for the layout of the probes. It is assumed that they will be connected by cables to a multiplexing readout located somewhere outside the detector.

10.6 HADRON CALORIMETER TIMING

The whole calorimeter will be timed using a single laser system so that every signal from every tower will arrive at the same time for an event that occurs at the centre of the CMS detector. Timing corrections will be performed at two places. The first is in the decoder box where the clock phasing can change the timing in 64 steps of 0.5 nsec each.

This will be used to synchronise the timing within a calorimeter unit, such as a wedge in the barrel calorimeter. The second adjustment place is in the DAQ where different modules can be timed to each other. The plan is to keep the optical readout fibres and other cables to a minimum length and apply the corrections electronically.

10.6.1 Time variation within a calorimeter wedge

The first step of the synchronisation process is to compute the time difference between various towers in a single module. This is accomplished as follows:

- a) Compute the time secondary particles will take to reach the layer of shower maximum for HB and HE, the first layer for HO and the front of HF. Here assume that the particles travel at the velocity of light (c).
- b) Compute the time the light signal takes to reach from the active region to the photo detectors. For this part the velocity of the signals in the fibres is measured to be about $0.5 c$.

The sum of step a and b will be stored within the computer so timing corrections can be applied in the decoder box to compensate for this difference.

The time variation inside a tower for HB and HE, from the various layers is of the order of 2 ns. This is due to the fact that particles travel at the velocity of light within the calorimeter, while the light signal travels inside the fibre at half that speed. The layers closest to the interaction point get the particles first, while their light signals takes the longest. This difference over the thickness of the calorimeter of one meter is about 1.5 ns. The time variation from tower to tower inside a single wedge is substantial. In HB the signal from $\eta = 0$ arrive about 15 ns later than the signal at $\eta = 1.5$. For HF the maximum time difference is smaller, of the order of 10 nsec. This difference in timing will be compensated in the decoder box as explained below. Similar timing correction will be applied for HO-B and HO-E. This time difference for HF is negligible, as the fibre cable length of each tower is about the same length.

10.6.2 Timing correction within a decoder box

Each decoder box gets one laser signal. Each tower is read by one photo detector pixel, where the output time of the signal can be varied inside the amplifier in 64 steps of 0.5 ns each for a total of 32 ns. This clock phasing is performed remotely by downloading the information via the field bus. This correction is applied so that the amplifier signals of each tower, if this was a real event, will come out at precisely the same time. This is where the photo detector timing variation will also be compensated. This means that the signal from the tower within a wedge that arrives the earliest will have the most delay by this clock phasing. The digital waveform decoder will read each tower so that each tower signal arrives at the appropriate delay as computed in chapter 10.6.1.

10.6.3 Overall timing

The same laser signal is sent to each decoder box. The laser fibre lengths will be cut to the required lengths, so that if the laser mimics a real event, every signal of each decoder box will arrive in synchronisation. This means the laser signal to all the HB and HE decoder boxes will arrive at the same time. The laser signal to all the HF decoder boxes will also arrive at a common time, but later to account for the difference in particle travel time. By adjusting DAQ clock phasing, the signals from every component will be synchronised. The blue LED will also be timed to be similar to the laser, so its signals will arrive at the decoder boxes at the same relative time as the laser.

10.6.4 Data acquisition and processing

During laser timing operations, a large number of channels are illuminated. Readout requirements range from the full system of about 16,000 channels to one of six possible

partitions corresponding to the two halves of the HB, HE and HF detectors where 2,000 to 3,500 channels are involved. Because of the volume of data and the need to take numerous different timing settings, the normal TriDAS system has been selected for data acquisition and processing. The exact division of control and data archiving functions between the on-line processor farm and the DCS general purpose computing services has yet to be determined. The laser trigger and the first-level trigger accept are derived from a counter on the 40 MHz system clock. An automatic second-level trigger accept forces readout at the same rate.

The operation of timing the 16,000 calorimeter channels with respect to each other will be done during the detector commissioning phase, before collider operations begin. Thus, there is no premium on achieving a high event rate. Most of the work will be done using the partitions corresponding to the two halves each of the HB, HE and HF detectors. For each event, a time frame of 16 consecutive readings is readout from each channel giving event records of 64 to 112 Kbytes (512 Kbytes for the whole detector). In the farm, histograms are accumulated and processed, and the operation is repeated for a different laser delay setting. The data set of results versus laser delay is then processed to determine the relative timing of the readout channels to each other.

This timing calibration is crucially dependent on the Timing and Trigger Control system stability. Using a sampling of channels, the stability of the results will be monitored continuously. Initially, this will be done many times per day to establish the size of diurnal variations. Subsequent monitoring intervals will depend on the outcome. Finally, it is anticipated that monitoring will continue into the operations phase and be done routinely between fills of the collider as one of a set of standard calibrations performed at the end of each store. Using 25 time settings and accumulating 1000 events per setting at a 1 kHz event rate requires 25 seconds. An event rate of 1 kHz for a small sample of channels (of order 256) allows 99% of the time between events for processing in the farm as the readout is capable of 100 kHz.

10.7 CALIBRATION WITH COLLIDER DATA

Proton-proton collider data taken in situ at the LHC will provide an additional calibration tool.

10.7.1 Calibration using taus

We may most simply use the pp collisions as a source of isolated hadrons whose energy may be measured in the magnetic field. This will enable the hadronic response of the calorimeter to be determined. One such source of isolated hadrons is taus from W and Z decays. Using a single hadron + missing E_T trigger, about 180 pions may be recorded for each HCAL tower in 10 fb^{-1} of data. Cuts on shower width and profile are required to select charged pions without accompanying π^0 s, but the resulting precision of the calibration is estimated to be 2% in each tower.[11]

10.7.2 Jet energy scale

Because pp interactions provide the only available source of jets, the jet energy scale must be determined from collision data. This can be done using a family of jet-balancing techniques.

Photon+jet balancing:

In this technique photons (or EM clusters from electromagnetically-fragmenting jets) are used to fix the jet energy scale relative to the EM scale (which can be determined from the Z resonance). Events with a single jet recoiling against the photon are selected, either by requiring that the photon and jet be almost back to back in azimuthal angle or by a veto on additional jets above some minimum E_T . The jet scale may then be determined as a function of the EM object E_T by minimising the projection of the missing E_T along the jet axis (the Missing E_T Projection Fraction or MPF). This is the primary jet calibration technique used by DØ, who have demonstrated 3% accuracy. It is also used as a cross-check by CDF. One disadvantage is that the maximum E_T photon which is attainable for any given luminosity is only about one third of the maximum jet E_T reached, since the photon cross section is much lower than that for jets. Consequently some extrapolation is always required at high E_T .

Z+jet balancing

We have looked at the possibility of extending this technique to Z+jet events. This will provide a cleaner signal than photons (though restricted to lower E_T). CDF have found that, with 100 pb^{-1} of data, Z+jet balancing gives a 5% check on the jet scale for $E_T < 50 \text{ GeV}$. We found[12] that 700 k Z+jet events (only one jet above 40 GeV E_T) could be accumulated per month at a luminosity of $10^{33} \text{ cm}^{-2} \text{ s}^{-1}$ sufficient to calibrate up to many hundreds of GeV in jet E_T .

Dijet balancing

This technique is used in DØ to transfer the calibration to very forward jets; a central jet (calibrated by one of the above techniques) is balanced against a forward jet whose calibration is to be determined. A similar procedure may be needed in CMS to calibrate the HF calorimeters.

Probably some combination of all the above techniques will be needed to determine the jet energy scale in CMS. All are demonstrated to work in a hadron collider environment, but all require Monte-Carlo to understand the possible biases (e.g. from jets below the minimum E_T cut or unclustered energy), since in all cases the entire mismeasurement is ascribed to the “probe jet”.

10.7.3 Dijet resonances

For direct verification of multijet mass reconstruction, e.g. for $W \rightarrow jj$ in high mass Higgs search and for $H \rightarrow bb$, it will be useful to have direct calibrations of dijet resolution and response using resonances of known mass.

W → jj in top decays

A proof of principle for this possibility is already present in CDF and DØ data, where the dijet mass of untagged jets in top events shows a clear peak near m_W . We find[12] that 45,000 double-tagged top events would be recorded each month at a luminosity of $10^{33} \text{ cm}^{-2} \text{ s}^{-1}$. A clear W-peak is visible when events consistent with top decay are selected, as was shown in chapter 1.5.1. The reconstructed $\langle m_W \rangle$ depends on the level of minimum bias pileup: it moves from 70 GeV → 60 GeV when $\langle n \rangle = 30$ pileup events are overlaid and a 1 GeV clustering threshold is added. This is not a problem with the calibration technique — it is exactly the kind of effect we wish to calibrate.

$$Z \rightarrow \bar{b}b$$

This will provide a handle on the energy scale of $\bar{b}b$ jets (should it prove to be different from light quarks). This signal should be visible in CDF/DØ data at the Tevatron by Run II and the rate at the LHC will be very large.

$$Z \rightarrow t+t-$$

Similarly, to determine the energy scale for tau-jets, the Z will provide a large signal at known mass.

References

- [1] Bertoldi et al, NIM 386 (1997) 301.
- [2] Virgil E. Barnes and Alvin T. Laasanen, "Proceedings of the First International Conference on Calorimetry in High Energy Physics", ed. D. F. Anderson, M. Derrick, H. E. Fisk, A. Para, and C. Sazama, World Scientific, (1991) 189.
- [3] Virgil E. Barnes, Alvin T. Laasanen and James A. Ross, "Proceedings of the Second International Conference on Calorimetry in High Energy Physics", ed. Antonio Ereditato, World Scientific, (1992) 195.
- [4] Qifeng Shen, "Proceedings of the Fifth International Conference on Calorimetry in High Energy Physics", ed. Howard A. Gordon and Doris Rueger, World Scientific, (1994) 302.
- [5] Virgil E. Barnes, "Proceedings of the Fifth International Conference on Calorimetry in High Energy Physics", ed. Howard A. Gordon and Doris Rueger, World Scientific, (1994) 338.
- [6] Solenoidal Detector Collaboration, "Technical Design Report", SDC Note SDC-92-201 (April, 1992).
- [7] "The CDF II Detector Technical Design Report", Fermilab-Pub-96/390-E (November, 1996).
- [8] Nural Akchurin, Virgil E. Barnes, James Freeman, Alvin T. Laasanen, Yasar Onel, Qifeng Shen and W. Wu, "CMS HCAL Calibration System -- Conceptual Design" CMS TN/96-040 (May 1996).
- [9] Nural Akchurin and Yasar Onel, "The PMT readout and Calibration issues for the SSCintCAL detector" GEM TN 92-184.
- [10] V.I.Kryshkin, L.K.Turchanovich, V.G.Vasil'chenko. Nucl. Instr. And Meth. A 381 (1996) 573.
- [11] R. Kinnunen, CMS HCAL meeting 3/15/97 and CMS-TN in preparation.
- [12] J. Freeman and W. Wu, Fermilab-TM-1984, 1996

TABLE OF CONTENTS

10.1 OVERVIEW.....	431
10.1.1 CALIBRATION AND MONITORING SYSTEMS.....	432
10.1.2 DISCUSSION OF CHOICE OF CALIBRATION TECHNIQUES.....	433
10.2 SPECIFICATIONS AND REQUIREMENTS (HB/HE/HO/HF).....	435
10.3 SOURCE CALIBRATIONS.....	436
10.3.1 DESIGN SPECIFICATIONS.....	436
10.3.2 LAYOUT.....	439
10.3.3 SYSTEM INTERFACES.....	443
10.3.4 DATA ACQUISITION AND PROCESSING.....	443
10.3.5 ACCESS, MAINTENANCE AND OPERATIONS.....	444
10.4 LASER CALIBRATION AND OTHER LIGHT INJECTION.....	444
10.4.1 SPECIFICATIONS.....	444
10.4.2 DESIGN.....	445
10.4.3 LAYOUT FOR HB, HE, HO AND HF.....	451
10.4.4 HF NORMALISATION.....	452
10.4.5 HF RADIATION DAMAGE MONITORING.....	453
10.4.6 OTHER HF NORMALISATION.....	453
10.4.7 DATA ACQUISITION AND PROCESSING.....	453
10.4.8 HF CALIBRATION AND MONITORING.....	454
10.5 OTHER SYSTEMS.....	457
10.6 HADRON CALORIMETER TIMING.....	457
10.6.1 TIME VARIATION WITHIN A CALORIMETER WEDGE.....	458
10.6.2 TIMING CORRECTION WITHIN A DECODER BOX.....	458
10.6.3 OVERALL TIMING.....	458
10.6.4 DATA ACQUISITION AND PROCESSING.....	458
10.7 CALIBRATION WITH COLLIDER DATA.....	459
10.7.1 CALIBRATION USING TAUS.....	459
10.7.2 JET ENERGY SCALE.....	459
10.7.3 DIJET RESONANCES.....	460
REFERENCES.....	462